CROATICA CHEMICA ACTA
CCACAA **80** (3-4) 313–324 (2007)

ISSN-0011-1643
CCA-3174
Original Scientific Paper

Surface Complexation of Selenite on Goethite: MO/DFT Geometry and Charge Distribution*

Tjisse Hiemstra, René P. J. J. Rietra, and Willem H. Van Riemsdijk**

Department of Soil Quality, Wageningen University, P.O. Box 47, NL 6700 AA Wageningen, The Netherlands

RECEIVED MARCH 1, 2007; REVISED APRIL 17, 2007; ACCEPTED APRIL 20, 2007

The adsorption of selenite on goethite (α-FeOOH) has been analyzed with the charge distribution (CD) and the multi-site surface complexation (MUSIC) model being combined with an extended Stern (ES) layer model option. The geometry of a set of different types of hydrated iron-selenite complexes has been calculated using Molecular Orbital / Density Functional Theory (MO/DFT). The optimized geometries have been interpreted with the Brown bond valence approach resulting in a set of ionic charge distribution values. After correction for dipole orientation effects, it results in the interfacial charge distribution coefficients that can be applied to the analysis of adsorption data. The use of theoretical CD values has the practical advantage of a reduction of the number of adjustable parameters. From a theoretical perspective, the CD values can constrain the model, revealing a surface speciation that can be tested experimentally. Modeling of the adsorption of SeO_3 in (pseudo-) monocomponent goethite systems, using the calculated CD values, has revealed the dominant presence of a bidentate surface species $\equiv(FeO)_2SeO$. The dominance of this surface species agrees with the interpretation of EXAFS measurements given in literature. The agreement supports the validity of the approach. To describe the adsorption at very low pH and a high loading, formation of an additional surface species is required in the modeling. The maximum contribution is about 20 % or less. In case of anion competition, as found in the PO_4-SeO_3 goethite system, the relative contribution increases. Analysis of the adsorption behavior in the PO_4-SeO_3 goethite systems revealed the probable nature of the additional surface complex, which is found to be a protonated monodentate surface complex $\equiv$FeOSeOOH. With the affinity constants derived, the CD model is able to describe the SeO_3 adsorption on goethite over a large range of pH, ionic strength, and loading conditions for a variety of goethite preparations. The CD model correctly predicts the proton co-adsorption of selenite and is able to describe the shift of the IEP upon addition of selenite.

Keywords
hematite
goethite
ferri-hydrite
HFO
singly coordinated
surface group
ligand
ATR-FTIR
selenite

INTRODUCTION

Metal (hydr)oxides play an important role in the regulation of the concentration of cations and anions in the environment. This is relevant for processes like bioavailability and environmental mobility. The ion adsorption behavior of metal (hydr)oxides can be described with surface complexation models (SCM). In general, ion adsorption leads to a change in the particle charge which will affect the binding energy.[1] Therefore, most SCM explicitly account for this variation using an electrostatic model. The lateral interactions can be successfully calculated with a SCM that applies the so-called smeared-out approximation of surface charge.[2]

* Dedicated to Professor Nikola Kallay on the occasion of his 65th birthday.

** Author to whom correspondence should be addressed. (E-mail: tjisse.hiemstra@wur.nl)

The electrostatic field radiated by a charged particle decays readily in the direction of the free solution due to the increased neutralization of the field by counter and co-ions, leading to a diffuse distribution pattern of the electrolyte ion charge.[1] The surface charge and the counter & co-ion charge form an electrostatic double layer. Near the surface, the gradient of the electrostatic potential is very large. For the calculation of the electrostatic energy of an ion in this field, the position of the ion charge in the gradient is very important. Therefore, structural details are required in the compact part in the double layer. Classically, this has been done for electrolyte ions. In the simplest -but physically realistic- approach, the electrolyte ions can only neutralize the field up to a certain minimum distance of approach.[3] Surface charge and the counter & co-ion charge remain separated by a layer, known as a Stern layer. Electrolyte ions can form outer-sphere complexes (ion pairs) that usually are located at the minimum distance of approach. The simplest approach is known as the Basic Stern (BS) model.[4] Recently, refinement of this double layer picture has been suggested,[5] based on the analysis of a consistent set of titration data obtained for goethite in the presence of various types of electrolyte ions comprising Li^+, Na^+, K^+, Cs^+, NO_3^-, and Cl^-.[6] The head end of the diffuse double layer (DDL) has found to be separated from the minimum distance of approach of electrolyte ions by a second Stern layer,[5] resulting in an Extended Stern (ES) layer model.[4] According to Hiemstra and Van Riemsdijk,[5] this double layer structure is due to the alignment of water molecules near the surface. In this water structure, electrolyte ions may only penetrate with stepwise changes in location. This molecular picture has been demonstrated by force measurements.[7,8] The alignment of water near the surface has recently been observed with X-ray reflectivity[9–11] and Sum Frequency Spectroscopy shows water structuring.[12–15] The measurements show increase in the ordering of water within a distance of about 0.7–0.9 nm, which is equivalent to about 2–3 layers of water molecules.[5]

The binding of an ion as outersphere complex is relatively weak. High affinity of ions for surfaces is generally related to the formation of innersphere complexes. In such a case, the ion will form some common ligands with the metal ions of the solid. In case of SeO_3^{2-} for example, bidentate complexes are formed[16] that have two ligands common with the surface. One of the oxygen ligands of the adsorbed SeO_3^{2-} species remains non-coordinated and will interact with interfacial water. The notion that only part of the coordination sphere is common with the surface has resulted in the formulation of the charge distribution (CD) model.[17] In this model, only a part of the ion charge is attributed to the surface. The remaining part is attributed to an electrostatic plane at some distance from the surface. In the first approach, the charge has been distributed based on the relative number of ligands of the adsorbed ion that are common with the surface. In the case of bidentate surface complex formation of SeO_3^{2-}, 2/3 of the ligands are common with the surface. This leads to a charge distribution in which about 2/3 of the ion charge is present at the surface plane.[18] This charge distribution is also found for the carbonate ion.[19] In case of the formation of a monodentate SeO_4 innersphere complex,[20,21] only one ligand is common with the surface and the other three oxygens are non-coordinating with the metal ions of the solid. Therefore, only one quarter of the charge of the SeO_4 ion is attributed to the surface.[22] The PO_4 ion will form bidentate complexes at the surface of goethite.[23] In that situation, half of the ligands and half of the ion charge is attributed to the surface. The above structural link between the distribution of charge in the inner Stern layer and the distribution of ligands has been demonstrated for a series of divalent oxyanions by Rietra *et al.*[18] In this simple approach, the charge is equally distributed over the ligands, known as a Pauling distribution of charge.[24]

In nature, ion charge is often asymmetrically distributed over the coordinating ligands. This asymmetry in the distribution of ion charge can be related to the variation in bond lengths as has been proposed by Brown.[25] In principle, the bond length is experimentally accessible with spectroscopic methods and can also be assessed with quantum chemical calculations. Molecular orbital (MO) calculations have recently been used to assess the ionic charge distribution in number of surface complexes.[5,26–28]

The thus calculated ionic charge distribution may differ from the interfacial CD value that is used in surface complexation modeling due to changes in the orientation of interfacial water molecules.[5] The charge distribution in an interface is affected by orientation of the water dipoles in the compact part of the double layer. The dipole orientation of water is able to partly reduce the electrostatic effects of the interfacial accumulation of charge. Due to dipole orientation, a small fraction of the surface charge is redistributed. The dipole contribution is generally relatively small ($\approx$ 0.17 valence units (v.u.) per unit of surface charge) but nevertheless it is often significant as has been shown for the adsorption of for instance $As(OH)_3$[26] and H_4SiO_4.[27]

The use of calculated CD values has the practical advantage that the number of adjustable parameters is reduced by a factor 2. Only one affinity constant has to be fitted per adsorbed species. Moreover, the approach creates a firm structural constraint in the modeling and can *in principle* be tested against spectroscopic information.

Recently, the adsorption of phosphate has been interpreted using CD coefficients that have been calculated according to the above approach.[28] The analysis

identified a bidentate (B) species as the main surface species for a large range of conditions. At high loading and a low pH, an additional phosphate surface complex is formed. The species, found from modeling, is a protonated monodentate (MH) complex. This interpretation differs from the surface speciation used in earlier interpretations where the formation of a protonated bidentate (BH) complex was assumed.[17] In the earlier interpretations, the CD value of the bidentate (B) complex was found using the Pauling bond valence analysis. A good description of the data was only found, if the charge of the protonated bidentate (BH) complex was significantly shifted, *i.e.* at least 0.5 valence units (v.u.), apparently due to proton binding. However, our recent molecular orbital calculations for this species[28] show that the shift of charge due to protonation is rather limited, only 0.19 v.u., which is significantly smaller than the shift of charge that is needed for a good description. A similar large shift of charge in case of protonation has also been assumed in our earlier work on the modeling of the adsorption of selenite.[29] Based on the recent experience with phosphate,[28] such a large shift can be questioned. In the present study, the CD values of various types of potentially possible selenite surface complexes will be calculated from the MO/DFT optimized geometry and corrected for dipole orientation effects. These CD values will be used as a constraint to model the adsorption behavior of selenite and to derive the surface speciation.

Quite some information is available with respect to the binding of selenite. The binding mode has been studied with extended X-ray absorption fine structure spectroscopy (EXAFS),[30–33] X-ray standing wave spectroscopy,[34] and attenuated total reflection Fourier transformed infrared spectroscopy (ATR-FTIR).[35] The adsorption of SeO_3 has been measured for a number of metal (hydr)oxides, *i.e.* for goethite,[35–42] hematite,[43] hydrous ferric oxide (HFO)[35] and for Al oxide.[44] In our study, we will focus on the binding to goethite. We will provide some new proton co-adsorption data for the adsorption of selenite to goethite. These data cover a relatively large range of SeO_3 loadings at two pH values. These data have been collected using a high solid-solution ratio as described in Rietra *et al*.[18] In the paper, we will first describe the geometry optimization approach and report the resulting CD values. This will be followed by the analysis of adsorption data.

MO/DFT CALCULATIONS

Quantum Chemical Calculations

The geometries of various types of complexes of iron selenite have been optimized using Spartan'04 software of Wavefunction.[45] First, we defined a cluster that serves as a template to mimic the goethite mineral (Figure 1a). The initial geometry of the octahedrons is set equal to the geometry found for goethite.[46] Additional protons (*d*-OH = 104 pm) have been added to obtain a zero-charged cluster, $Fe_2(OH)_6(OH_2)_4$ ($z = 0$). To define the various SeO_3 complexes, one or two of the OH_2 ligands on top that are repre-

Table I. The distances (pm) in the geometry of selenite complexes hydrated with water molecules (*n*-H_2O) coordinating to respectively the common and the free ligands, calculated with the DFT-BP86 model

	≡$(FeO)_2SeO$ (B)	≡$(FeO)_2SeOH$ (BH)	≡$FeOSeO_2$ (M)	≡FeOSeOOH (MH)	Exp.
n-H_2O	2+3[a]	2+2	1+4	1+4	
O-Se[b]	174.7	169.2	181.8	172.6	–
O-Se[b]	174.9	172.0	–	–	–
Se-O[b]	174.7	–	169.2	169.1	–
Se-O[b]	–	–	174.0	–	–
Se-OH[b]	–	187.6	–	185.0	–
Fe-O	206.7±0.3	214.0±1.1	208.1	209.3	196[c]
Fe-Se	335.6±0.1	342.3±1.2	353.5	355.5	338[d]
R_o	187.1	186.1	185.3	187.3	181.1[e]
$n_0 + n_{H0}$[f]	–1.34+2	–0.96+2	–0.90+1	–0.59+1	
$n_1 + n_{H1}$[f]	–0.66+0	–1.04+1	–1.10+0	–1.41+1	

[a] The number of coordinating water molecules with respectively the common oxygen(s) or with the free ligand(s) of the complexes.
[b] Se-O and SeOH refer to the bond of Se with the free O/OH ligand and O-Se to the bond with the common oxygen.
[c] Distance present in the goethite structure without relaxation.
[d] EXAFS study reporting *d* (Fe-Se) = 338 pm[16] and a coordination number CN = 2.1.
[e] Average R_0 for Se^{IV} in minerals.[25]
[f] The n_0 and n_1 values represent the partial charge of SeO_3 ($n_0 + n_1 = -2$) attributed to the 0- and 1-plane. These coefficients are calculated combining the Brown bond valences and the charge of the oxygens ligands placed in the electrostatic plane. The n_{H0} and n_{H1} values represent the charge of additional protons that are located in respectively the 0- and 1-plane at formation from the components.

sentative for the singly coordinated surface groups at the 110 face of goethite, have been replaced to form respectively a double corner bidentate or a single corner monodentate complex. An additional proton is added to the free ligand of SeO_3 in case of protonation of the surface complex. The complexes defined are representative for the surface complexes $\equiv(FeO)_2SeO$ (B), $\equiv(FeO)_2SeOH$ (BH), $\equiv FeOSeO_2$ (M) and $\equiv FeOSeOOH$ (MH). To mimic the hydration of the complexes, extra water molecules have been defined that interact with the O or OH ligands of Se *via* H bridges. The number of added water molecules (n_{H_2O}) is given in Table I. In addition, some calculations have been done on non-hydrated structures.

The geometry optimizations were done using density functional theory (DFT). Pseudo potentials, defined in Spartan'04 as LACVP+** were used. This set comprises the 6–31+G** basis set for the main group elements H-Ar. The + and ** signs refer to the use of respectively diffuse and polarization functions. For Se^{IV}, the final geometry was calculated with the gradient corrected BP86 model. It is assumed that the Fe ions have a high spin electron configuration.

RESULTS AND DISCUSSION

Geometry

The geometries of four different types of Fe-Se complexes have been optimized. These complexes are representative for the formation of a bidentate $\equiv(FeO)_2SeO$, a protonated bidentate $\equiv(FeO)_2SeOH$, a monodentate $\equiv FeOSeO_2$, and a protonated monodentate $\equiv FeOSeOOH$ surface complex. The relevant distances in the complexes are given in Table I. The optimized geometry of the bidentate complex $\equiv(FeO)_2SeO$ is shown in Figure 1b.

The geometries of Table I can be interpreted in terms of a charge distribution using the Brown bond valence concept. According to Brown and Altermatt,[25] the bond valence s is related to the distance R as:

$$s = e^{-(R-R_0)/B} \qquad (1)$$

in which B is a constant and R_0 is the element specific parameter. Brown and Altermatt[25] used the value B = 37 pm. The value of R_0 is chosen such that the sum of the bond valences around the Se^{IV} ion corresponds to the formal valence (z = +4). The various R_0 values calculated for the optimized structures (Table I) are systematically larger than the R_0 value found for minerals. This is also found in previous MO/DFT studies for PO_4,[28,47] CO_3,[5] As^{III},[26,48,49] As^{V},[26,50] and Si.[5,27] Application of Eq. (1) results in a set of ionic charge distribution values. These values are related to the formation reactions of the different complexes. The formation of B, BH, and MH complexes can be defined respectively with the reactions:

$$2\equiv FeOH^{-1/2} + SeO_3^{-2}(aq) + 2H^+(aq) \leftrightarrow \equiv(FeO)_2^{-1+\Delta z_0}SeO^{\Delta z_1} + 2H_2O(l); \quad K_B \qquad (2)$$

$$2\equiv FeOH^{-1/2} + SeO_3^{-2}(aq) + 3H^+(aq) \leftrightarrow \equiv(FeO)_2^{-1+\Delta z_0}SeOH^{\Delta z_1} + 2H_2O(l); \quad K_{BH} \qquad (3)$$

$$1\equiv FeOH^{-1/2} + SeO_3^{-2}(aq) + 1\ H^+(aq) \leftrightarrow \equiv FeO^{-1/2+\Delta z_0}SeO^{\Delta z_1} + 1\ H_2O(l); \quad K_M \qquad (4)$$

$$1\equiv FeOH^{-1/2} + SeO_3^{-2}(aq) + 2H^+(aq) \leftrightarrow \equiv FeO^{-1/2+\Delta z_0}SeOOH^{\Delta z_1} + 1\ H_2O(l); \quad K_{MH} \qquad (5)$$

in which Δz_0 and Δz_1 are the interfacial charge distribution coefficients expressing the overall change of charge of the 0- and 1-plane relatively to the charge of the reference species ($\equiv FeOH^{-1/2}$) used in the formation reactions. In other words, the sum $\Sigma\Delta z_i$ is equal to the total charge of ions adsorbed. The ionic charge distribution

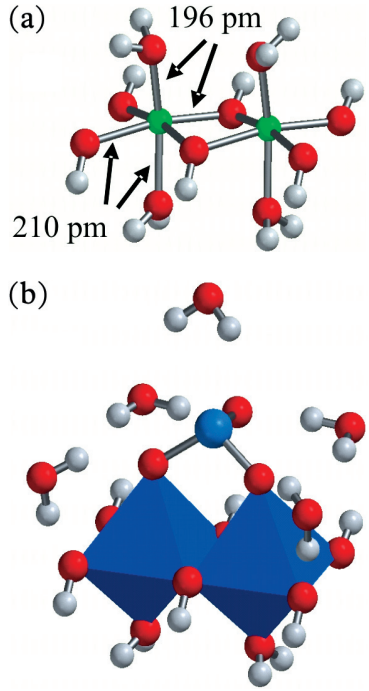

Figure 1. (a) The initial geometry of two Fe^{III} octahedra with distances and angles representative for goethite. (b) The optimized geometry of a hydrated bidentate complex (MO/DFT/BP) of SeO_3 formed at the exchange of two H_2O ligands on top of the octahedra that are representative for the protonated singly coordinated surface groups of the 110 face of goethite. All ions in the structure were allowed to relax, except the lower part of both Fe octahedra, *i.e.* $Fe_2(OH)_6(OH_2)_2$.

Table II. The relevant distances (pm) in the geometry of a non-hydrated, non-protonated selenite bidentate complex ≡$(FeO)_2SeO$ (B) optimized with various MO/DFT models. The bond lengths have been interpreted with the Brow bond values approach resulting in the ionic charge allocation ($n_0 + n_{H0}$, $n_1 + n_{H1}$)

Method	Local	EDF1	BP86	BLYP	B3LYP	Exp
O-Se[a]	176.8	177.3	178.3	178.8	175.4	170[b]
O-Se[a]	176.8	177.3	178.3	178.9	175.4	170[b]
Se-O[a]	166.9	168.4	168.7	169.3	166.6	170[b]
Fe-O	189.9±0.1[c]	199.6±0.0	198.0±0.0	200.9±0.0	196.7±0.0	196[d]
Fe-Se	318.3±0.0[c]	334.7±0.0	330.7±0.0	336.5±0.0	334.7±0.0	338[e]
R_0	183.8	184.8	185.5	186.1	182.9	181.1[f]
n_0+n_{H0}[g]	–1.58+2	–1.55+2	–1.57+2	–1.57+2	–1.55+2	
n_1+n_{H1}[g]	–0.42+0	–0.45+0	–0.43+0	–0.43+0	–0.45+0	

[a] Se-O refers to the bond of Se with the free O ligand and O-Se to the bond with the common oxygen.
[b] EXAFS data for Se^{IV} adsorbed to goethite $d_{Se\text{-}O}$ = 170 pm.[16]
[c] Average value and variation
[d] Distance present in the goethite structure without relaxation.
[e] EXAFS study reporting d(Fe-Se) = 338 pm and a coordination number CN = 2.1.[16]
[f] Average R_0 for Se^{IV} in minerals.[25]
[g] The n_0 and n_1 values represent the partial charge of SeO_3 ($n_0 + n_1 = -2$) attributed to the ligands of the 0- and 1-plane. These coefficients are calculated combining the Brown bond valences and the charge of the oxygens ligands placed in the electrostatic plane. The n_{HO} and n_{H1} values represent the charge of additional protons that are located in respectively the 0- and 1-plane.

Table III. The ionic charge distribution values of SeO_3^{-2} for complexes that are hydrated or non-hydrated

	Hydrated[a]		non-Hydrated[b]	
Species	n_0+n_{H0}[e]	n_1+n_{H1}[e]	n_0+n_{H0}[e]	n_1+n_{H1}[e]
≡$(FeO)_2SeO$	–1.34+2	–0.66+0	–1.56+2±0.01[c]	–0.44+0±0.01
≡$(FeO)_2SeOH$	–0.96+2	–1.04+1	–1.04+2±0.02	–0.96+1±0.02
≡FeOSeOOH	–0.59+1	–1.41+1	–0.66+1±0.02[d]	–1.34+1±0.02[d]

[a] From table I based on the BP86 model
[b] Average values obtained for the Local, EDF1, BP86, BLYP and B3LYP model
[c] Standard deviation of the data obtained with the different models used
[d] In the average value the Local MO/DFT model result has been excluded
[e] The n_0 and n_1 values represent the partial charge of SeO_3 ($n_0 + n_1 = -2$) attributed to the 0- and 1-plane. These coefficients are calculated combining the Brown bond valences and the charge of the oxygens ligands placed in the electrostatic plane. The n_{H0} and n_{H1} values represent the charge of additional protons that are located in respectively the 0- and 1-plane.

coefficients ($n_0 + n_{H0}$, $n_1 + n_{H1}$), related to the charge of SeO_3^{-2} (n_0, n_1) and additional protons (n_{H0}, n_{H1}), are given in Table I. Correction of these values for the dipole orientation effects will lead to the interfacial CD values (Δz_0, Δz_1), as is discussed later.

To illustrate the importance of the presence of hydration water and the sensitivity of the calculated ionic CD values to the use of various DFT methods, we did a number of calculations for non-hydrated structures. The results are shown in Table II for the non-protonated ≡$(FeO)_2SeO$ complex. The calculated ionic CD values vary slightly (about ±0.02 v.u.) with the MO/DFT method used. A more important difference arises from the presence of hydration water. For the BP86 model, the CD values for the hydrated and non-hydrated structure of ≡$(FeO)_2SeO$ differ considerably, *i.e.* 0.22 v.u., showing the importance of the presence of hydration water. The effect of hydration is less strong for the protonated complexes MH (0.07 v.u.) and BH (0.08 v.u.) as can be seen from the data given in Table III.

In our calculations, the lower part of the octahedra (Figure 1b) has been fixed to the geometry found in goethite. For phosphate, it has been shown[5] that full relaxation results in a relatively small change of the CD value (0.03 v.u.), illustrating that the CD is not particularly sensitive to the precise geometry of the octahedrons. For this reason, it may be assumed that the ionic CD values calculated using a cluster with only two Fe octahedra are a reasonable approximation of the CD values for a hydrated crystal surface.

In conclusion, the expected uncertainty in the calculated ionic CD values is probably less than about 0.05 v.u.

Interfacial CD Values

As mentioned above, the ionic bond valences ($n_0 + n_{H0}$, $n_1 + n_{H1}$), obtained from the optimized geometries, can be transformed into the overall interfacial charge distribution values by correcting for dipole effects. The introduction of charge in the interface due to the adsorption of ions leads to orientation of the water dipoles in the compact part of the double layer[5] and is linked to a dipole energy change. The dipole energy depends on the potential fall in the Stern layer and can be interpreted as an electrostatic feedback on the introduction of ion charge at the surface.

The overall electrostatic energy is related to the net charge that is introduced in the Stern layer region. The change of charge in respectively the 0- and 1–plane can be formulated as:[5]

$$\Delta z_0 = n_0 + n_{H0} - \phi(n_0 + n_{H0} + \Sigma n_{ref} z_{ref}) \qquad (6)$$

and

$$\Delta z_1 = n_1 + n_{H1} + \phi(n_0 + n_{H0} + \Sigma n_{ref} z_{ref}) \qquad (7)$$

in which n_0 and n_1 represent the ion charge and n_{H0} and n_{H1} the additional proton(s) that is/are introduced in respectively the 0- and 1-plane. The values of Δz_0 and Δz_1 represent the overall charge attribution to the mentioned planes and the symbol ϕ is a proportionality factor ($\phi \approx 0.17 \pm 0.03$). The dipole change is to be calculated relatively to the neutral reference state of surface groups (see Hiemstra and van Riemsdijk[5]). For this reason, the factor $\Sigma n_{ref}\ z_{ref}$ is introduced in the dipole correction term $\phi(n_0 + n_{H0} + \Sigma n_{ref}\ z_{ref})$ in Eqs. (6) and (7). In this term, n_{ref} is the number and z_{ref} the charge of the reference group(s). The dipole correction can be used to transform the above calculated ionic charge (Table I) into the overall interfacial charge distribution coefficients (Δz) as given in Table IV.

The above calculated interfacial charge distribution coefficients (Δz_0, Δz_1) are very different. The net charge introduced in the 0-plane ranges from about $\Delta z_0 = 0.4$ to 1.0 v.u. This charge is particularly important for the pH dependency of the adsorption. The charge attributed to the 1-plane varies from about $\Delta z_1 = -0.7$ to 0.0 v.u. This charge is particularly important in determining the internal competition of species as a function of loading and has particularly influence on the shape of the adsorption isotherm. The relatively large variation in coefficients implies that the description of the adsorption data may be sensitive to the surface species chosen to describe the adsorption behavior. We note that comparison of the calculated CD values of $\equiv(FeO)_2SeO$ and $\equiv(FeO)_2SeOH$ (Table IV) shows that protonation of the bidentate complex leads to a considerable redistribution of charge, *i.e.* 0.41 v.u. In case of protonation of the monodentate complex, we also observe a relatively large shift (0.31 v.u.). This value is considerably larger than previously found for the protonation of the PO_4 bidentate complex[28] (0.20 v.u.) and that of arsenate[26] (0.11 v.u.). This value is rather close to the value (0.5 v.u.) that we successfully used previously[29] in our modeling. It suggests that the use of $\equiv(FeO)_2SeOH$ may lead to a good description of the data. This will be tested in the modeling section of this paper.

Spectroscopy

To our knowledge, the first EXAFS measurement on adsorbed ions was done for SeO_3^{2-} on goethite.[16] To explain the Fe-Se distance, Hayes *et al.*[16] suggested that SeO_3^{2-} was present as a double corner bidentate surface complex. The formation of bidentate complexes was later confirmed.[31] For hydrous ferric oxide (HFO), a smaller Fe-Se distance has been observed, which has be-

Table IV. The ionic charge distribution values ($n_0 + n_{H0}$, $n_1 + n_H$) of SeO_3^{-2} adsorbed according to the reactions, Eqs. (2)–(5), and the overall charge distribution coefficients (Δz_0, Δz_1) after correction for dipole orientation. The log *K* values for the adsorption reaction of selenite and phosphate refer to respectively Eqs. (2)–(5) and Eqs. (8) and (9)

Species	n_0+n_{H0}	n_1+n_{H1}	$\Delta z_{0\ (calc)}$	$\Delta z_{1(calc)}$	Δz_2	log $K^{(c)}$
$\equiv(FeO)_2SeO$[(a)]	–1.34+2	–0.66+0	+0.72	–0.72	0	24.86±0.02[(d)]
$\equiv(FeO)_2SeOH$[(a)]	–0.96+2	–1.04+1	+1.03	–0.03	0	–
$\equiv FeOSeO_2$[(a)]	–0.90+1	–1.10+0	+0.20	–1.20	0	–
$\equiv FeOSeOOH$[(a)]	–0.59+1	–1.41+1	+0.43	–0.43	0	19.65±0.05
$\equiv(FeO)_2PO_2$[(b)]	–1.45+2	–1.65+0	+0.46	–1.46	0	30.29±0.05
$\equiv FeOPO_2OH$[(b)]	–0.76+1	–2.24+1	+0.28	–1.28	0	27.98±0.03

[(a)] CD values calculated in this study
[(b)] CD values are taken from Rahnemaie *et al.*[28]
[(c)] The log *K* values for SeO_3 and PO_4 are found by fitting respectively the SeO_3 and PO_4 adsorption data of the competition experiment of Hingston *et al.*[36] in an alternating procedure (see text). In case of a fit of the SeO_3 monocomponent data of Hingston *et al.*, Hayes *et al.*, and Campbell and Eick,[36,39,42] one finds log $K_B = 24.53 \pm 0.04$ and log $K_{MH} = 19.59 \pm 0.25$ (see text).
[(d)] The best estimate and the standard deviation

en interpreted as the formation of a bidentate complex bound by the edge of a Fe octahedron. Recently, it has been shown with X-ray standing wave (XSW) spectroscopy[34] that a smaller Fe-Se distance can also be representative for double corner complexes in case of rotation of Fe octahedra as has been found at the 100 face of hematite. It illustrates that caution is required in the interpretation of EXAFS data.[34]

Modeling

The primary charge of goethite has been described assuming the presence of two types of reactive sites, *i.e.* singly ($\equiv FeOH^{-1/2}$) and triply ($\equiv Fe_3O^{-1/2}$) coordinated surface groups. The proton affinity of both groups has been set equal to the value of the PZC.[51] For ion pair formation, the parameter set of Rahnemaie *et al.*[28] has been used (Table V). These parameters have been derived by simultaneously fitting of an internally consistent set of titration data,[6] collected for various types of electrolyte ions. As mentioned in the introduction, the modeling showed that the head end of the DDL is separated from the location where the electrolyte ions reside as ion pair. It implies that we use an Extended Stern layer model. The inner and outer Stern layer capacitances were found to be very similar.[5] Due to the uncertainty in the determination of the precise value of the outer Stern layer capacitance ($C_2 \approx 0.7$–1.4 F/m^2)[5], the value of C_2 has been set equal to the value of the inner Stern layer. This can be considered as an arbitrary choice, but it can be shown that the model results are rather insensitive to the precise value of outer capacitance C_2. Recently, Sverjensky[52] has increased the value of the outer capacitance of the triple layer model arbitrarily from the original value of 0.2 F/m^2 to a value that is set equal to the capacitance of the inner layer, resulting in the same double layer setup.

In our previous SeO_3 modeling study,[29] we have analyzed the $SeO_3 - PO_4$ interaction measured by Hingston *et al.*,[36] using a previous interpretation of the PO_4 adsorption behavior (the presence of a protonated and a non-protonated bidentate surface complex). The adsorption of phosphate has recently been studied over a very large range of conditions.[28] As mentioned above, analysis of the data, using a series of surface species with *a priori* calculated CD values revealed the presence of two surface species, *i.e.* a bidentate $\equiv(FeO)_2PO_2$ and protonated monodentate $\equiv FeOPO_2OH$ surface species. Note that this combination of surface species is different from earlier interpretations. The adsorption reactions can be formulated as:

$$2\equiv FeOH^{-1/2} + PO_4^{-3}(aq) + 2H^+(aq) \leftrightarrow \equiv(FeO)_2^{-1+\Delta z_0}PO_2^{\Delta z_1} + 2H_2O(l); \quad K_5 \qquad (8)$$

$$1\equiv FeOH^{-1/2} + PO_4^{-3}(aq) + 2H^+(aq) \leftrightarrow \equiv FeO^{-1/2+\Delta z_0}PO_2OH^{\Delta z_1} + 1\ H_2O(l); \quad K_6 \qquad (9)$$

in which $\Delta z_0 + \Delta z_1 = -1$ v.u., *i.e.* the sum of the change of charge due to adsorption of two protons (+2 v.u.) and the trivalent phosphate ion (–3 v.u.). For our goethites, the log K values are log $K_B = 29.72$ and log $K_{MH} = 27.63$.[28]

The phosphate adsorption of the goethite of Hingston *et al.*[36] is slightly larger than found for our goethites. In a first approach, we have adjusted the affinity constants by fitting the data of the monocomponent system giving log $K_B = 30.10 \pm 0.09$ and log $K_{MH} = 27.71 \pm 0.05$ ($R^2 = 0.99$). We note that an apparent difference in affinity might be due to differences in the total number of available sites[29] (determined by the total surface area, the relative contribution of the crystal faces and corresponding site densities), since site saturation effects may occur at high loading.

In the present modeling of the SeO_3 adsorption, we will use the calculated CD values as a constraint to reveal the surface speciation. All surface species are initially allowed in the model. The surface speciation and corresponding affinity constants will be derived by fitting. In a first approach, we have used the adsorption data from a series of monocomponent SeO_3 adsorption experiments published by various authors,[36,39,42] all re-

Table V. Charge allocation (Δz) and the affinity constants (log K) of monovalent ions reacting with singly ($\equiv FeOH^{-1/2}$) and triply ($\equiv Fe_3O^{-1/2}$) coordinated surface groups having a site density of respectively 3.45 and 2.7 nm^{-2}.[28] The capacitance of the Stern layers of the Extended Stern layer model are set equal, *i.e.* $C_1 \equiv C_2 = 0.92$ F m^{-2} (see text)

Ions	Δz_0	Δz_1	Δz_2	Log K
H^+	+1	0	0	+ 9.2
Na^+	0	+1	0	– 0.61
K^+	0	+1	0	– 1.74
H^+-NO_3^-	+1	–1	0	+9.2 –0.70[(a)]
H^+-Cl^-	+1	–1	0	+9.2 –0.44[(a)]

[(a)] Note that in the case of $H^+NO_3^-$ and H^+Cl^- the first value (+9.2) corresponds to affinity constant of H^+ ion, while the second values (–0.70 and –0.44) correspond to affinity constants of NO_3^- and Cl^- ions, respectively.

ferring to goethites with a relatively high specific surface area. In these systems, the added SeO_3 is equivalent with a potential loading in the range of 0.07 – 3.1 – 4.6 μmol/m^2. Two other data sets[38,40] were excluded from our modeling since these were inconsistent with the data sets chosen. Modeling showed that the SeO_3 adsorption data set of Hayes,[39] referring to a systems with a relatively high pH (pH ≈ 9–12) and a low loading (0.07 μmol/m^2), could be described well using only one surface species which turned out to be the bidentate species ≡$(FeO)_2SeO$ (Eq. (2)). This species is also identified as surface species with EXAFS.[16] The data sets with a high loading (3.1–4.6 μmol/m^2), comprising data at low pH[36,42] could not be described well at low pH using only the bidentate species. However, the introduction of an additional species that is protonated increases the quality of the fit. Unfortunately, no significant difference was found for the quality of the fit assuming the additional presence of a protonated bidentate surface species ≡$(FeO)_2SeOH$ (R^2 = 0.94) or the presence of a protonated monodentate species ≡FeOSeOOH (R^2 = 0.94), *i.e.* it is difficult to decide, based on the analysis of this data set, which additional surface species is active. An important reason for the insensitivity is the relatively low contribution of this additional species to the overall adsorption. This can be illustrated by the difference in the uncertainty of the fitted log K values. The combination of ≡$(FeO)_2SeO$ (B) and ≡FeOSeOOH (MH) results in respectively log K_B = 24.43 ± 0.04 and log K_{MH} = 19.6 ± 0.3. The combination with the two bidentate surface species, *i.e.* ≡$(FeO)_2SeO$ and ≡$(FeO)_2SeOH$ gives respectively log K_B = 24.43 ± 0.04 and log K_{BH} = 30.3 ± 0.9. In both cases, the uncertainty in the log K value of the protonated surface species (BH and MH) is relatively large in contrast to the log K of the dominant non-protonated bidentate (B) surface species. No clues are found for the presence of a non-protonated monodentate species (≡$FeOSeO_2$).

It may be expected that the relative presence of any protonated species will be higher in the SeO_3-PO_4 competition data set of Hingston *et al.*[36] because of the large negative charge on the particles as result of the binding of PO_4. This negative charge will stimulate the presence of protonated species. We have used the log K values, derived from the monocomponent systems, to predict the adsorption of PO_4 and SeO_3 in the competition experiments. A significantly better description is found for the combination B & MH (R^2 = 0.92) than for the combination B & BH (R^2 = 0.79).

The quality of the description of the data of Hingston *et al.*[36] using the B and MH species can be increased by deriving the log K values of SeO_3 and PO_4 *via* fitting of the SeO_3 and PO_4 data of the experiment (R^2 = 0.978) using an alternating approach in which the log K values for SeO_3 are found from the SeO_3 competition data and that for PO_4 from the PO_4 competition data. This set of log K values is given in Table IV. The log K value found for the SeO_3 bidentate surface complex of the goethite in this experiment is slightly larger (≈0.3 log K units) than found for the other goethite systems that we analyzed. As mentioned above, this has also been found for the phosphate binding of the goethite of Hingston *et al.*[36] in comparison to the data of Rahnemaie *et al.*[28] In this respect, consistency exists.

The competitive adsorption data and the modeling results are shown in Figure 2. In Figure 2a, we have indicated for the highest and the lowest SeO_3 adsorption the amount of SeO_3 present as non-protonated bidentate species, ≡$(FeO)_2SeO$ (dotted line). The difference with the solid line illustrates the contribution of the protonated surface species ≡FeOSeOOH (MH). The bidentate ≡$(FeO)_2SeO$ surface species is fully dominant in most situations. Only a small contribution of the ≡FeOSeOOH surface species is found at low pH (pH < 5).

Despite a slightly higher affinity of SeO_3 for the goethite of Hingston *et al.*, the set of log K values derived (Table IV) is nevertheless able to describe the other mentioned SeO_3 adsorption data[36,39,42] reasonably

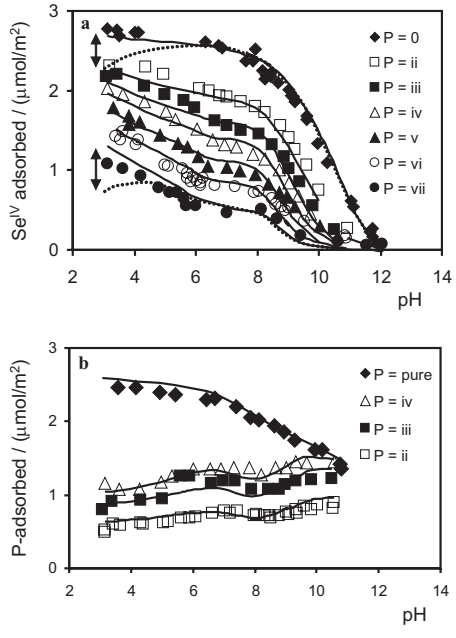

Figure 2. (a) The adsorption of selenite on goethite (ρ = 4.36 g/L, A = 81 m^2/g) in 0.1 mol dm^{-3} NaCl (20 °C) for systems with various levels of phosphate. The initial PO_4 concentrations are (ii) = 0.39, (iii) = 0.77, (iv) = 1.29, (v) = 2.58, (vi) = 5.16, and (vii) = 12.9 mmol dm^{-3}. The initial SeO_3 concentration is 1.02 mmol dm^{-3}. (b) The adsorption of phosphate corresponding to the systems of (a), and the PO_4 adsorption without selenite on goethite (4.36 g/L, A = 81 m^2/g) in 0.1 mol dm^{-3} NaCl (20 °C) with an initial P concentration of 1.29 mmol dm^{-3}. Data are from Hingston *et al.*[36] The lines are calculated with the parameters of Tables IV and V. For the highest and lowest SeO_3 loading, not only the total SeO_3 adsorption is given (full line), but also the amount present as a non-protonated SeO_3 complex (≡$(FeO)_2SeO$) is given (dotted line). The vertical arrows indicate the significance of the protonated surface species (≡FeOSeOOH).

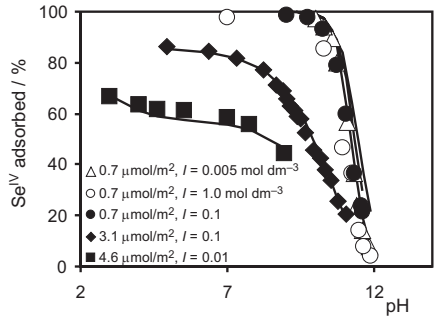

Figure 3. The pH-dependent adsorption of selenite on goethite for systems with different selenite loadings at various electrolyte levels. The data for the systems with a loading of 0.07 μmol/m^2 in $NaNO_3$ are from Hayes *et al.*[39] (ρ = 30 g/L, A = 52 m^2/g, SeO_3-initial = 0.1 mmol dm^{-3}). The system with a loading of 3.1 μmol/m^2 in 0.1 mol dm^{-3} NaCl is from Hingston *et al.*[36] (see Figure 2a). The system with a loading of 4.6 μmol/m^2 in 0.01 mol dm^{-3} $NaNO_3$ is from Campbell and Eick[42] (ρ = 2.5, A = 87 m^2/g, SeO_3-initial =1.0 mmol dm^{-3}). The lines are calculated with the model parameters of Tables IV and V.

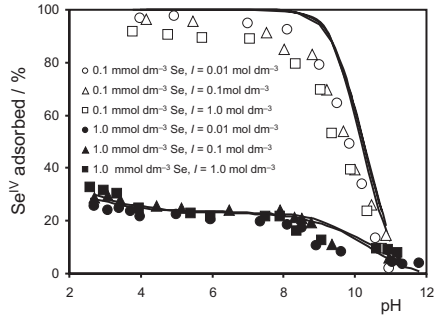

Figure 4. The adsorption edges of selenite on goethite (ρ = 4 g/L, A = 21.8 m^2/g) at three NaCl background electrolyte concentrations for two initial SeO_3 concentrations (C = 0.1 and 1 mmol dm^{-3}). Data are from Su and Suarez.[35] The lines are calculated with the CD model parameters of Tables IV and V.

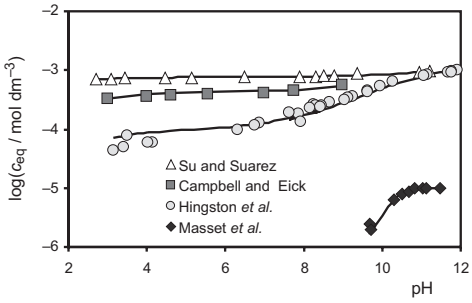

Figure 5. The logarithm of the equilibrium concentrations found in various SeO_3-goethite systems as function of pH. The conditions in the systems are for Su and Suarez:[35] ρ = 4 g/L, A = 21.8 m^2/g, SeO_3-initial = 0.1 mmol dm^{-3}, 0.1 mol dm^{-3} NaCl (see Figure 4), for Campbell and Eick:[42] ρ = 2.5 g/L, A = 87 m^2/g, SeO_3-initial = 1.0 mmol dm^{-3}, 0.01 mol dm^{-3} $NaNO_3$ (see Figure 3), for Hingston *et al.*:[36] ρ = 4.36 g/L, A = 81 m^2/g, SeO_3-initial = 1.02 mmol dm^{-3}, 0.1 mol dm^{-3} NaCl (see Figure 2a) and for Masset *et al.*:[41] ρ = 2 g/L, A = 20 m^2/g, SeO_3-initial = 0.01 mmol dm^{-3}, 0.1 mol dm^{-3} KNO_3. The lines are calculated with the CD model parameters given in Tables IV and V.

well as shown in Figure 3. Moreover, also the SeO_3 adsorption data[35,41] for goethite preparations with a low specific surface area (≈21 ± 1 m^2/g) could also be well-described with the same set of log K values as shown in Figure 4 and Figure 5. In the latter figure, the equilibrium concentrations are given, showing the span of concentrations covered in the various experiments. For the conditions present in the lower right corner of Figure 5, the adsorption is only due to the binding of the bidentate species (B). In the upper left corner, the protonated monodentate complex (MH) contributes too.

Electrophoretic-mobility

Su and Suarez[35] have also measured the electrophoretic-mobility of goethite in the absence and presence of SeO_3. The measurements show a shift in the IEP as function of the SeO_3 loading (Figure 6). Although differences exist at higher SeO_3 concentrations between the calculated d-plane potential and measurement, the shift of the IEP is rather well predicted as shown in Figure 6. At the highest SeO_3 loading, the measured electrophoretic-mobility, expressed in the zeta potential (open squares) and the calculated potential at the head end of the DDL (line) deviate for unknown reasons.

Proton Co-adsorption

When a negatively charged ion approaches a variable-charge surface, the surface groups will react with the uptake of protons. In general, this process is the main reason for the experimentally observed proton co-adsorption. We have measured the proton co-adsorption of selenite by adding SeO_3 to a goethite suspension with a rather high solid-solution ratio (10.1 g/L) while keeping the pH value constant by adding acid, using the method described in Rietra *et al.*[18] The experiment covers a larger range of SeO_3 additions than previously published.[18] Calculations show that in all cases 99.8 % or more of the added Se is adsorbed. It implies that the added amount of SeO_3 in Figure 7 can be interpreted as adsorbed. The parameters of Tables IV and V have been used to predict the proton co-adsorption.

As shown in Figure 7 (lines), the model correctly predicts the experimental observations. Since proton co-adsorption is thermodynamically linked to the pH dependency of the adsorption,[53–55] it implies that the model correctly predicts the pH dependency of the SeO_3 adsorption. Moreover, our calculations show that in the experimental range the SeO_3 adsorption is fully dominated by the presence of the non-protonated bidentate species with a negligible contribution of the other surface species. In that case, the calculated proton co-adsorption is fully determined by only the charge distribution,[18] since all other parameters are constrained by structural implications or determined independently from experimental data. The value of the formation constant of ≡$(FeO)_2SeO$

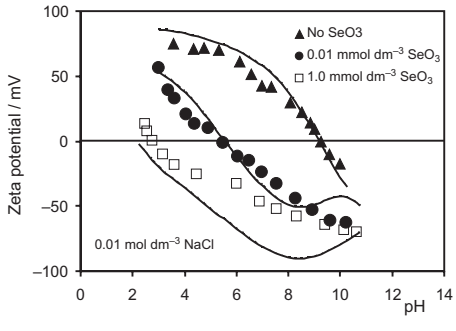

Figure 6. The zeta potential of goethite (ρ = 0.2 g/L, A = 21.8 m^2/g) in 0.01 mol dm^{-3} NaCl as function of pH at different initial concentrations of SeO_3. The lines represent the potential at the head end of the DDL (extended Stern layer model), calculated with the model parameters of Tables IV and V.

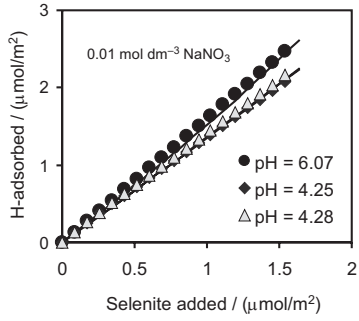

Figure 7. The co-adsorption of protons upon addition of selenite to a goethite suspension with initially ρ = 10.1 g/L, A = 96.4 m^2/g in 0.01 mol dm^{-3} $NaNO_3$ for different pH values. The lines are calculated with the model parameters of Tables IV and V.

(log K_B) is totally irrelevant in the calculation of the proton co-adsorption, as long as the model calculates that the added amount of SeO_3 approximates the amount adsorbed. In other words, the CD value is the only model parameter determining the proton co-adsorption if one surface species is active. The CD value regulates the interaction of the charge of the adsorbed ion with the surface groups. Increase of the value of the surface charge attribution (Δz_0) leads to the presence of more negative charge at the surface that will respond by binding extra protons to the unoccupied surface groups. The correct prediction of the proton co–adsorption and hence the pH dependency, implies that the calculated CD value is accurately derived from the MO/DFT optimized geometry and dipole correction.

General Discussion

The modeling has revealed the dominant binding of SeO_3 as bidentate complex, in agreement with spectroscopy. The interpretation of modeling with respect to the minor species at high loading and low pH is less certain. Spectroscopic verification is desired. At present, no such data are available. Identification of the minor species can probably be done best in an oxyanion competition experiment at low pH like the above discussed PO_4-SeO_3 system. A model interpretation at high loading is in general less firm because the ordinary electrostatic regulation of the ion competition is increasingly influenced by physical site competition effects. At high loading, the type and contribution of crystal faces, corresponding site densities and the potential variation in affinity of these sites becomes more relevant in the modeling but is in effect uncertain. Moreover, in our statistical formulation of mass action,[17] the probability function $(\theta_{FeOH})^m$, defined as the relative concentration of unoccupied surface sites (mole fraction of the reference species) with m = 2 for bidentate formation, is a simplification.[56,57] The mass action factor $(\theta_{FeOH})^2$ is applicable to a microscopic adsorption site with two surface groups that react as a unit, whereas at the 110 face of goethite the surface groups are present in rows where the microscopic site, formed by combinations of two adjacent surface groups, continuously overlaps leading to another mixing entropy factor with $m < 2$.[57]

In the modeling of our previous SeO_3 study,[29] we have used only bidentate complexes. The CD value of ≡$(FeO)_2SeO$ (B) was estimated using the Pauling rule (Δz_0 = 2–1.33 = +0.67 v.u., Δz_1 = –0.67 v.u.) and for the ≡$(FeO)_2SeOH$ (BH) complex, we assumed an additional shift of charge of 0.5 v.u. toward the surface, which was supposed to be due to the protonation of the free oxygen ligand of ≡$(FeO)_2SeO$ (Δz_0 = +1.07 v.u., Δz_1 = –0.07 v.u.). The CD values calculated in the present study show that these previous estimates of the CD values are very close to the present CD values that are based on the MO/DFT optimized geometry and dipole correction, *i.e.* Δz_0 = +0.72 v.u., Δz_1 = –0.72 v.u. (B) and Δz_0 = +1.03 v.u., Δz_1 = –0.03 v.u. (BH). It suggests that the combination of species (B and BH) previously used might be seen as realistic. Despite this correspondence, our detailed modeling nevertheless suggests that another combination of surface species is active, *i.e.* ≡$(FeO)_2SeO$ (B) and ≡FeOSeOOH (MH). How come?

We have shown above that the adsorption of SeO_3 is mainly determined by the presence of the non-protonated bidentate complex ≡$(FeO)_2SeO$ (B). Only a small contribution of a second species is required in the modeling at high loading and low pH. In the present modeling, we could not derive from the monocomponent systems the identity of this surface species. The choice of ≡FeOSeOOH (MH) as additional species has been based on the analysis of the PO_4–SeO_3 competition data. In this analysis, we used for phosphate the combination ≡$(FeO)_2PO_2$ (B) and ≡$FeOPO_2OH$ (MH) which is based on our very recent evaluation of the PO_4 binding mechanism,[28] whereas in our previous analysis[29] we used only bidentate complexes for phosphate adsorption. This difference is important, because the competition experiments refer to systems with a very high loading where

physical site competition becomes important, apart from the, – usually dominant –, electrostatic competition. Since both factors are different in the treatment of phosphate in the present approach, we have come to another conclusion with respect to the possible identity of the protonated species, *i.e.* the presence of a protonated monodentate surface complex (MH).

CONCLUSIONS

The above can be summarized in a series of conclusions:

- The charge distribution of the SeO_3 bidentate surface complex can be calculated from the MO/DFT optimized geometry in combination with a double layer correction.
- In the MO/DFT geometry optimization, hydration of the complex is essential, if the aim is to predict the charge distribution for a surface complex present at the solid-solution interface. Application of different MO/DFT models to find the CD from the geometry reveals a variation in the calculated CD value of about ± 0.02 v.u.
- Application of calculated CD values in the interpretation of the adsorption of SeO_3 reveals the dominance of a bidentate surface complex, in full agreement with spectroscopic observations. At low pH and high SeO_3 loading, an additional surface species is present. The relative presence of this species increases in case of competition with phosphate ions. Modeling suggests the formation of a protonated monodentate surface complex under these conditions. In a monocomponent system at high loading and very low pH, its contribution is estimated to be 20 % or less.
- The CD model is able to describe the SeO_3 adsorption on goethite over a large range of pH, ionic strength, and loading conditions for a variety of goethite preparations using independently calculated CD coefficients.
- The CD model correctly predicts the proton co-adsorption of selenite and is able to describe the shift of the IEP upon addition of selenite.

Acknowledgement. – Part of this work was funded by the FUNMIG project (516514, F16W-2004).

REFERENCES

1. N. Kallay and S. Žalac, *J. Colloid Interface Sci.* **230** (2000) 1–11.
2. M. Borkovec, *Langmuir* **13** (1997) 2608–2613.
3. O. Stern, *Z. Electrochem.* **30** (1924) 508–516.
4. J. Westall and H. Hohl, *Adv. Colloid Interface Sci.* **12** (1980) 265–294.
5. T. Hiemstra and W. H. Van Riemsdijk, *J. Colloid Interface Sci.* **301** (2006) 1–18.
6. R. Rahnemaie, T. Hiemstra, and W. H. Van Riemsdijk, *J. Colloid Interface Sci.* **293** (2006) 312–321.
7. R. M. Pashley and J. N. Israelachvili, *J. Colloid Interface Sci.* **101** (1984) 511–523.
8. J. N. Israelachvili and H. Wennerstrom, *Nature* **379** (1996) 219–225.
9. M. F. Toney, J. N. Howard, J. Richer, G. L. Borges, J. G. Gordon, O. R. Melroy, D. G. Wiesler, D. Yee, and L. B. Sorensen, *Surf. Sci.* **335** (1995) 326–332.
10. P. Fenter and N. C. Sturchio, *Prog. Surf. Sci.* **77** (2004) 171–258.
11. J. G. Catalano, C. Park, Z. Zhang, and P. Fenter, *Langmuir* **22** (2006) 4668–4673.
12. M. S. Yeganeh, S. M. Dougal, and H. S. Pink, *Phys. Rev. Lett.* **83** (1999) 1179–1182.
13. S. Kataoka, M. C. Gurau, F. Albertorio, M. A. Holden, S. M. Lim, R. D. Yang, and P. S. Cremer, *Langmuir* **20** (2004) 1662–1666.
14. V. Ostroverkhov, G. A. Waychunas, and Y. R. Shen, *Phys. Rev. Lett.* **94** (2005) 046102.
15. Y. R. Shen and V. Ostroverkhov, *Chem. Rev.* **106** (2006) 1140–1154.
16. K. F. Hayes, A. L. Roe, G. E. Brown, Jr., K. Hodgson, J. O. Leckie, and G. A. Parks, *Science* **238** (1987) 783–785.
17. T. Hiemstra and W. H. Van Riemsdijk, *J. Colloid Interface Sci.* **179** (1996) 488–508.
18. R. P. J. J. Rietra, T. Hiemstra, and W. H. Van Riemsdijk, *Geochim. Cosmochim. Acta* **63** (1999) 3009–3015.
19. T. Hiemstra, R. Rahnemaie, and W. H. Van Riemsdijk, *J. Colloid Interface Sci.* **278** (2004) 282–290.
20. H. Wijnja and C. P. Schulthess, *J. Colloid Interface Sci.* **229** (2000) 286–297.
21. D. Peak and D. L. Sparks, *Environ. Sci. Technol.* **36** (2002) 1460–1466.
22. R. P. J. J. Rietra, T. Hiemstra, and W. H. van Riemsdijk, *J. Colloid Interface Sci.* **240** (2001) 384–390.
23. M. I. Tejedor-Tejedor and M. A. Anderson, *Langmuir* **6** (1990) 602–611.
24. L. Pauling, *J. Am. Chem. Soc.* **51** (1929) 1010–1026.
25. I. D. Brown and D. Altermatt, *Acta Crystallogr., Sect. B* **41** (1985) 244–247.
26. M. Stachowicz, T. Hiemstra, and W. H. Van Riemsdijk, *J. Colloid Interface Sci.* **302** (2006) 62–75.
27. T. Hiemstra, M. O. Barnett, and W. H. Van Riemsdijk, *J. Colloid Interface Sci.* **310** (2007) 8–17.
28. R. Rahnemaie, T. Hiemstra, and W. H. Van Riemsdijk, *Langmuir* **23** (2007) 3680–3689.
29. T. Hiemstra and W. H. Van Riemsdijk, *J. Colloid Interface Sci.* **210** (1999) 182–193.
30. K. F. Hayes and J. O. Leckie, *J. Colloid Interface Sci.* **115** (1987) 564–572.
31. A. Manceau and L. Charlet, *J. Colloid Interface Sci.* **168** (1994) 87–93.
32. A. L. Foster, G. E. Brown, and G. A. Parks, *Geochim. Cosmochim. Acta* **67** (2003) 1937–1953.
33. D. Peak, *J. Colloid Interface Sci.* **303** (2006) 337–345.
34. J. G. Catalano, Z. Zhang, P. Fenter, and M. J. Bedzyk, *J. Colloid Interface Sci.* **297** (2006) 665–671.

35. C. Su and D. L. Suarez, *Soil Sci. Soc. Am. J.* **64** (2000) 101–111.
36. F. J. Hingston, A. M. Posner, and J. P. Quirk, *Diss. Faraday Soc.* **52** (1971) 334–342.
37. D. D. Hansmann and M. A. Anderson, *Environ. Sci. Technol.* **19** (1985) 544–551.
38. L. S. Balistrieri and T. T. Chao, *Soil Sci. Soc. Am. J.* **51** (1987) 1145–1151.
39. K. F. Hayes, C. Papelis, and J. O. Leckie, *J. Colloid Interface Sci.* **125** (1988) 717–726.
40. P. C. Zhang and D. L. Sparks, *Environ. Sci. Technol.* **24** (1990) 1848–1856.
41. S. Masset, F. Monteil-Rivera, L. Dupont, J. Dumonceau, and M. Aplincourt, *Agronomie* **20** (2000) 525–535.
42. J. L. Campbell and M. J. Eick, *Clays Clay Miner.* **50** (2002) 336–341.
43. M. Duc, G. Lefevre, and M. Fedoroff, *J. Colloid Interface Sci.* **298** (2006) 556–563.
44. C. H. Wu, S. L. Lo, and C. F. Lin, *Colloids Surf., A* **166** (2000) 251–259.
45. Anonymous Spartan '04 Wavefunction Inc.; Irvine CA USA, 2004.
46. J.-L. Hazemann, J. F. Berar, and A. Manceau, *Mater. Sci. Forum* **79** (1991) 821–826.
47. K. D. Kwon and J. D. Kubicki, *Langmuir* **20** (2004) 9249–9254.
48. N. L. Zhang, P. Blowers, and J. Farrell, *Environ. Sci. Technol.* **39** (2005) 4816–4822.
49. A. C. Q. Ladeira, V. S. T. Ciminellie, H. A. Duarte, M. C. M. Alves, and A. Y. Ramos, *Geochim. Cosmochim. Acta* **65** (2001) 1211–1217.
50. D. M. Sherman and S. R. Randall, *Geochim. Cosmochim. Acta* **67** (2003) 4223–4230.
51. T. Hiemstra, P. Venema, and W. H. Van Riemsdijk, *J. Colloid Interface Sci.* **184** (1996) 680–692.
52. D. A. Sverjensky, *Geochim. Cosmochim. Acta* **69** (2005) 225–257.
53. M. J. Perona and J. O. Leckie, *J. Colloid Interface Sci.* **106** (1985) 65–69.
54. R. P. J. J. Rietra, T. Hiemstra, and W. H. Van Riemsdijk, *J. Colloid Interface Sci.* **229** (2000) 199–206.
55. T. Hiemstra and W. H. Van Riemsdijk, in: *Encyclopaedia of Surface and Colloid Science*, 1 ed., Marcel Dekker, Inc., New York, USA, 2002, pp. 3773–3799.
56. M. M. Benjamin, *Environ. Sci. Technol.* **36** (2002) 307–313.
57. R. A. LaViolette and G. D. Redden, *Environ. Sci. Technol.* **36** (2002) 2279–2280.

SAŽETAK

Površinsko kompleksiranje selenita na getit: MO/DFT geometrija i raspodjela naboja

Tjisse Hiemstra, René P. J. J. Rietra i Willem H. Van Riemsdijk

Adsorpcija selenita na getit (*a*-FeOOH) analizirana je modelom raspodjele naboja (*charge distribution,* CD) i modelom površinskog kompleksiranja raznovrsnih površinskih mjesta (*multi-site surface complexation,* MUSIC*)* kombiniranim s proširenim modelom Sternovog (*extended Stern*, ES) sloja. Geometrija različitih tipova hidratiziranih željezo-selenit kompleksa izračunana je korištenjem *Molecular Orbital / Density Functional Theory* (MO/DFT). Optimizirane geometrije interpretirane su Brownovim pristupom valentnoj vezi rezultirajući nizom vrijednosti ionske raspodjele naboja. Nakon korekcije za utjecaje orijentacije dipola, dobiveni su koeficijenti međupovršinske raspodjele naboja, koji se mogu primijeniti na analizu adsorpcijskih podataka. Uporaba teorijskih vrijednosti CD ima praktičnu prednost zbog smanjenoga broja prilagodljivih parametara. Iz teorijske perspektive, vrijednosti CD mogu ograničiti model, određujući površinsku specijaciju koja se može eksperimentalno ispitati. Modeliranje adsorpcije SeO_3 u (pseudo-) monokomponentnom sustavu getita, koristeći izračunane vrijednosti CD, otkrilo je dominantnu prisutnost bidendatne površinske vrste $\equiv(FeO)_2SeO$. Dominacija ove površinske vrste u skladu je s interpretacijom EXAFS mjerenja danih u literaturi. Dobiveno slaganje podupire prikladnost odabranog pristupa. Za opisivanje adsorpcije pri jako niskom pH i visokom opterećenju, pri modeliranju je potrebno formiranje dodatne površinske vrste. Maksimalni doprinos je 20 % ili manje. U slučaju kompeticije aniona, kao što je pronađeno u sustavu PO_4-SeO_3 getit, relativni doprinos raste. Analiza adsorpcijskog ponašanja u sustavu PO_4-SeO_3 getit otkrila je vjerojatnu prirodu dodatnog površinskog kompleksa, za koji je pronađeno da je protonirani monodendatni površinski kompleks $\equiv$FeOSeOOH. S izvedenim konstantama afiniteta, CD model omogućuje opis adsorpcije SeO_3 na getit u širokom rasponu pH i ionske jakosti te uvjeta opterećenja za niz preparata getita. CD model ispravno predviđa koadsorpciju protona na selenit i može opisati pomak IEP po dodatku selenita.